EPR Investigation of Compound I in *Proteus mirabilis* and Bovine Liver Catalases: Formation of Porphyrin and Tyrosyl Radical Intermediates

Anabella Ivancich,[‡,§,||] Hélène Marie Jouve,[§,⊥] Bernard Sartor,[▽] and Jacques Gaillard*[,‡,§]

Département de Recherche Fondamentale sur la Matière Condensée, SCIB/SCPM, and Département de Biologie Moléculaire et Structurale, BMC, CEA-Grenoble, 17 Rue des Martyrs, F-38054 Grenoble, France, and Institut de Biologie Structurale Jean-Pierre Ebel, Laboratoire d' Enzymologie Moléculaire, CEA/CNRS, 41 Rue des Martyrs, F-38027 Grenoble, France

Received April 16, 1997; Revised Manuscript Received April 28, 1997[⊗]

ABSTRACT: Compound I of *Proteus mirabilis* and bovine liver catalases (PMC and BLC, respectively) were studied combining EPR spectroscopy and the rapid-mix freeze−quench techniques. Both enzymes, when treated with peroxyacetic acid, form a catalytic intermediate which consists of an oxoferryl porphyrin π-cation radical. In PMC this intermediate is semistable, and an unexpected reversible equilibrium under pH influence takes place between two forms of compound I with different coupling between the oxoferryl and the porphyrin π-cation radical. At acid pH, one form has a ferromagnetic character as in *Micrococcus luteus* compound I. At neutral pH, another form with a much smaller coupling, reminiscent of the horse radish peroxidase compound I, is detected. The approximate midpoint, estimated for these changes in the range $5.3 < \text{pH} < 6.0$, approaches the pK_a value of an histidyl residue. The residues possibly involved in the transformation are discussed in terms of the known structure of PMC compound I. The EPR spectrum of BLC compound I (pH 5.6), obtained in the millisecond time scale (40 ms), also showed a mixture of two forms which, most probably, correspond to two different magnetic exchange interactions, as in the case of PMC. Taken together, the low-temperature electronic absorption and the EPR spectra of BLC compound I formed in the 0.04−15 s range show that the porphyrin π-cation radical disappears and, instead, a tyrosyl radical is formed. ENDOR experiments confirm our previously estimated hyperfine couplings to the $C_{2,6}$ and $C_{3,5}$ ring protons and the β-methylene protons of the purported tyrosyl radical. Candidates for such a tyrosyl radical are discussed in connection with the possible electron transfer pathways between the heme active site and the NADPH cofactor.

Catalases (hydrogen peroxide: hydrogen peroxide oxidoreductase, EC 1.11.1.6) are redox enzymes responsible for the disproportionation of hydrogen peroxide into water and molecular oxygen (Deisseroth & Dounce, 1970). These metalloproteins can be found in aerobic organisms and play a crucial role in prokaryotic and eukaryotic cell detoxification. The crystal structures of five heme catalases, isolated from bovine liver, *Penicillium vitale*, *Micrococcus luteus*, *Proteus mirabilis*, and *Escherichia coli*, have been solved at high resolution (reviewed in Bravo et al., 1997). All of these structures reveal that heme catalases are tetramers, and each of the four active sites consists of a pentacoordinated-iron protoporphyrin IX prosthetic group with a tyrosinate axial ligand. Some of these structures (bovine liver catalase (BLC[1]), *Proteus mirabilis* catalase (PMC)) show a NADPH cofactor tightly bound at the periphery of each subunit.

The heme active site of native catalase is known to be in a high-spin ferric state (Fe^{3+}) and can convert to compound I intermediate state due to a two-electron oxidation by hydrogen peroxide (Schonbaum & Chance, 1976; Fita & Rossmann, 1985). One electron is removed from the iron atom which thus forms the oxoferryl moiety (Fe^{4+}═O) with the oxygen atom from the hydrogen peroxide molecule and the second electron is removed from the porphyrin resulting in a π-cation radical ($por^{\circ+}$). The first EPR and ENDOR evidence for compound I was reported for MLC treated with peroxyacetic acid, a pseudosubstrate wich produces a very stable compound I in this bacterial enzyme. From these studies, it was concluded that the EPR signal of MLC I corresponds to a porphyrin π-cation radical in ferromagnetic exchange interaction with the oxoferryl moiety (Benecky et al., 1993). Very recently, we have reported EPR experiments of BLC also treated with peroxyacetic acid and we have showed that, at variance with MLC EPR data, the signal at $\mathbf{g} = 2$ well agrees with a tyrosyl radical (Ivancich et al., 1996).

For the so-called catalatic cycle, the compound I is converted back to the native (ferric) state due to a subsequent two-electron reduction by a second molecule of hydrogen peroxide (Schonbaum & Chance, 1976). Alternatively, under

[†] A.I. acknowledges a CTE contract from CEA (Grenoble) and a postdoctoral fellowship from CONICET (Argentina).

* Corresponding author. Tel: (33) 04 76 88 35 98. Fax: (33) 04 76 88 50 90. E-mail: gaillard@drfmc.ceng.cea.fr.

[‡] Département de Rechereche Fondamentale sur la Matière Condensée.

[§] Joint first authorship.

[||] Permanent address: Instituto de Física de Líquidos y Sistemas Biológicos (CONICET), Universidad Nacional de La Plata, 59 No. 789. cc. 565, 1900 La Plata, Argentina. E-mail: ivancich@iflysib1.unlp.edu.ar.

[⊥] Institut de Biologie Structurale Jean-Pierre Ebel.

[▽] Département de Biologie Moléculaire et Structurale.

[⊗] Abstract published in *Advance ACS Abstracts,* August 1, 1997.

[1] Abbreviations: BLC, bovine liver catalase; PMC, *Proteus mirabilis* catalase; MLC, *Micrococcus luteus* catalase; CcP, cytochrome *c* peroxidase; APX, ascorbate peroxidase; LiP, lignin peroxidase; CPO, chloroperoxidase; CcP, cytochrome *c* peroxidase; BLC I, PMC I, MLC I, APX I, CPO I, CcP I or LiP I, BLC, PMC, MLC, APX, CPO, CcP, or LiP compound I; HpH I, high pH PMC I; LpH I, low pH PMC I; RNR, ribonucleotide reductase; PSII, photosystem II; AF, antiferromagnetic.

S0006-2960(97)00886-6 CCC: $14.00

a steady and low flow of hydrogen peroxide as it can occur under physiological conditions (Chance et al., 1979), compound I is reduced by an unidentified donor to another intermediate state, compound II, which is proposed to consist only of an oxoferryl moiety by analogy to peroxidases (Chuang et al., 1989). Compound II cannot end the catalatic cycle as compound I but it can either react with another H_2O_2 molecule to give an inactive compound III or be reduced to the native enzyme by endogenous or exogenous one-electron donor (Deisseroth & Dounce, 1970). Thus, the formation of compounds II and III in catalases implies an inactivation of the enzyme (Lardinois, 1995) with the subsequent accumulation of H_2O_2, that is deleterious for the organism as in inflammation, aging or some cancers (Halliwell & Gutteridge, 1984; Vuillaume, 1987). For NADPH binding catalases, a mechanism has been proposed by which the enzyme is protected against inactivation by preventing compound II formation or by reducing it while oxidizing NADPH to $NADP^+$ (Kirkman et al., 1987; Hillar & Nicholls, 1992). Only very recently, the crystal structures of both intermediates, compound I and compound II, of PMC have been solved (Gouet et al., 1996). No major protein conformational changes could be observed between the native, compound I, and compound II states, although the heme iron, which is 0.1 Å below the heme plane in the native state, was observed to move upward in compound I (0.3 Å above the heme plane) and back into the heme plane in compound II (Gouet et al., 1996). An unexpected anion binding could occur at a site 18 Å below the heme iron in compound I but not in compound II. Its role remains unclear.

This work presents comparative studies on compound I of the bacterial catalase isolated from *P. mirabilis* and the catalase extracted from bovine liver. In both cases compound I was induced by treatment with peroxyacetic acid. EPR data on PMC I not only agree well with the model of a porphyrin π-cation radical in exchange interaction with the oxoferryl moiety, but also this interaction shows an unprecedented pH dependence. From the results of rapid-mix freeze−quench experiments combined with EPR measurements, it appears that both the typical porphyrin-based as well as the tyrosyl radical intermediates are formed in BLC at different time scales. ENDOR measurements on BLC constitute further evidence to the assignment of the protein-based radical to a tyrosine residue. Possible candidates for this tyrosyl radical are proposed. The differences in reactivity with the peroxyacetic acid of the mammalian and the bacterial catalases are discussed in relation to their structures, as well as the implications on the catalytic cycle.

EXPERIMENTAL PROCEDURES

The catalase of *Proteus mirabilis* PR, a peroxide resistant mutant which overexpresses the catalase (Buzy et al., 1995), was purified as described previously (Jouve et al., 1989). BLC in crystalline solution (Boehringer-Manheim, Germany) was dialyzed against 0.1 M Tris-maleate buffer, pH 7.5, during 48 h and further purified by FPLC chromatography (Pharmacia, France) over an ion exchange D-Zephyr column (Sepracor, France). Fractions with final a A_{405}/A_{280} ratio of *ca.* 0.90 were selected for the EPR measurements. Catalase samples used for EPR and absorption measurements were concentrated by using a Centricon 30 microconcentrator (Amicon) to *ca.* 0.25 mM, and 5% glycerol was added to the buffer. For the treatment of catalase with peroxyacetic acid, stock solutions of peroxyacetic acid (42 mM) were prepared by dilution of the commercial peroxyacetic acid (32% solution, Merck) in 0.1 M Tris, adjusting the final pH to 4.3 with HCl. These solutions were incubated for 1 h at 4 °C with trace amounts of diluted catalase (Jones & Middlemiss, 1972). Typically, 120 μL of 0.25 mM catalase sample were mixed with 50 μL of 42 mM peroxyacetic acid directly into the EPR tube at 0 °C and quickly frozen (15 s) with liquid nitrogen. After the peroxyacetic acid stock solution (pH 4.3) was mixted with native BLC in 0.1 M Tris-maleate buffer (pH 7.5), the resulting pH of the compound I sample was measured to be 5.6. For the ENDOR measurements, native BLC samples were deuterated for 72 h by repeated cycles of concentration and resuspension, as well as overnight incubation in deuterated 0.1 M Tris-maleate buffer, corrected pD 7.8.

PMC I samples were prepared as described above for BLC. For the pH variations in PMC I, an initial pH of 6.8 was obtained by mixing 200 μL of 0.135 mM native PMC (0.1 M Tris-HCl buffer pH 7.2) with 25 μL of 42 mM peroxyacetic acid stock solution whose pH was adjusted at 3.3. Then, the pH was changed by addition of small amounts of diluted citric acid or 1 M Tris base in the PMC I samples. All of the pH values were measured immediately after thawing the samples.

Concentrations in tetrameric catalase were estimated spectrophotometrically using an absorption coefficient ϵ_{405} of 3.24×10^5 M^{-1} cm^{-1} for BLC (Samejima & Yang, 1963) and ϵ_{406} of 2.987×10^5 M^{-1} cm^{-1} for PMC (Jouve et al., 1984; Buzy et al., 1995).

The free tyrosyl radical sample used for the EPR power saturation studies was generated by irradiation, with a 240 W UV lamp (254 nm wavelength) of 10 mM tyrosine solution (12.5 mM sodium borate buffer, pH 10). The EPR tube with the tyrosine solution was irradiated for 20 min at 77 K.

Low-temperature (10 K) electronic absorption spectra were recorded with a Cary spectrometer. Catalase samples (0.2 mL) were held in plexiglas cuvettes (0.2 mm optical path) and immersed in a cryostat (SCM-TBT, France) cooled by circulation of cold helium gas. The reaction of catalase with peroxyacetic acid (the final pH of the mixture was 5.6 and 5.3 for BLC and PMC, respectively) was done directly into the plexiglas cuvettes at 0 °C and quickly (15 s) immersed in liquid nitrogen. The catalase samples contained 30% glycerol in order to form a good optical glass. Baseline correction on the spectra was done using a polynomial fit.

EPR measurements were performed with an X-band Varian E109 spectrometer, and the spin concentration of the BLC radical was determined by comparison of the double integrals of the EPR signal with that of a ferredoxin sample of known concentration (Moulis et al., 1996).

ENDOR masurements were performed with a Bruker ER200 X-band spectrometer equipped with an ER200-NB cavity. The radiofrequency power was supplied from an ENI (Rochester, NY) A500 amplifier (3−35 MHz, 500 W) driven by a frequency generator (Adret Electronique, France) (300 Hz/180 MHz). The magnetic field was measured by an Bruker NMR Gausmeter ER035M, and the frequency was monitored with a microwave frequency counter, Hewlett-Packard 5350B. Data acquisition was performed by a homemade program running on a Hewlett-Packard computer.

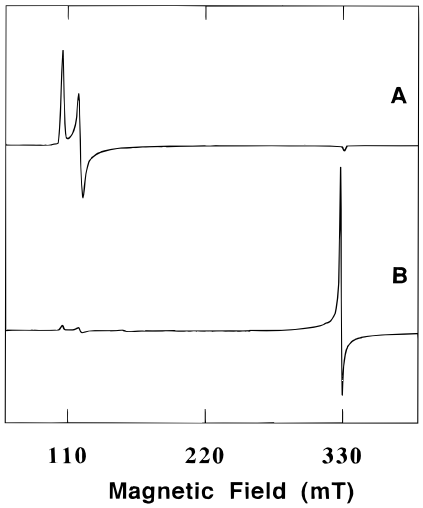

FIGURE 1: 4.2 K EPR spectra of the native (A) and the peroxyacetic acid-treated PMC (B). Concentration in tetrameric catalase: 0.120 mM in 0.1 M Tris-HCl buffer, pH 7.2, 5% glycerol (A); in (B), same conditions except peroxyacetic acid concentration was 4.6 mM and final pH 6.8. EPR conditions: microwave frequency, 9.22 GHz; microwave power, 1 mW; modulation frequency, 100 kHz; modulation amplitude, 1 mT.

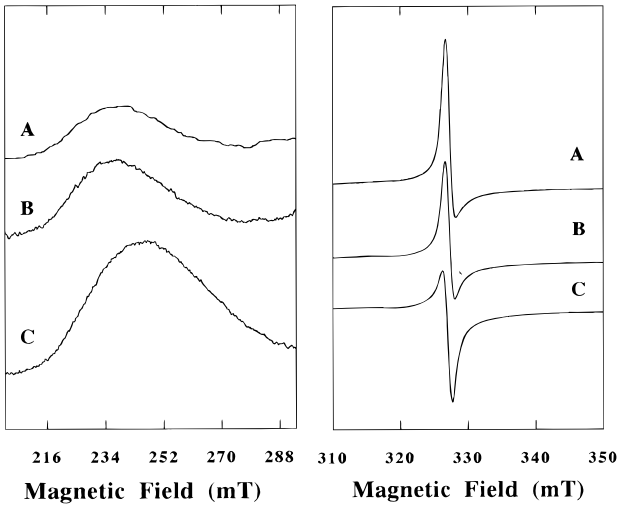

FIGURE 2: pH effect on the EPR signals of PMC I, at low field (right) and high field (left). The final pH values were (A) pH 6.8, (B) pH 6.0, and (C) pH 5.3. The spectra in A are an expansion of Figure 1B. For the spectrum B, 20 μL of 0.05 M citric acid, pH 4.5 was added to the sample in A. For the spectra C, an additional 20 μL of 0.05 M citric acid was added to the sample B. EPR conditions were as in Figure 1 with the gain on the left was 10 times higher than that used on the right part.

The rapid-mix freeze−quench experiments were done with a BioLogic MIXCOM apparatus. The syringes containing catalase samples and the peroxyacetic acid stock solution as well as the mixing chamber were all refrigerated by a water bath (T = 10 °C). A series of delay lines of different volumes (from 20 to 150 μL) were used to vary the mixing time. Typically, 48 μL of catalase (pH 7.5) and 18 μL of 42 mM peroxyacetic acid (pH 4.3) were mixed, and the final pH of the sample was 5.6. The syringes were driven by a stepper motor, and a series of delay lines of different volumes (from 20 to 150 μL) were used to vary the mixing time. The samples were sprayed through a nozzle of 0.2 mm directly into a funnel connecting to the EPR tubes, all immersed into an isopentane bath at 143 K. To estimate the final time at which the reaction of catalase and peroxyacetic acid was stopped, two values were taken in account: one due to the passage from the mixing chamber to the nozzle and another for the flight between the nozzle and the isopentane bath surface. The parameters used in this estimation were those provided for the apparatus, as the flow rate, the volume of sample delivered by the syringes, the diameter of the nozzle, the volume of the delay lines; the distance between the nozzle and the bath surface was 4 cm. Since the freezing at the surface of the isopentane bath is not instantaneous, an extra term contributing to the final time mentioned is needed; for this we used the calibration obtained from the reaction of myoglobin and sodium azide (Appleyard et al., 1994). The error on this estimated value is ±10 ms.

RESULTS

EPR of PMC I. pH Effect on the Oxoferryl Porphyrin π-Cation Radical. The 9 GHz EPR spectrum of PMC at 4.2 K is shown in Figure 1, both for the native and the peroxyacetic acid-treated catalase samples. The native EPR signal of the bacterial catalase, at pH 7.2 (Figure 1A), has the typical pattern of a rhombically distorted high-spin ferric heme, with resonance absorption lines extending between $\mathbf{g}$ = 6 and g = 2. The observed values of the effective g-tensor for the EPR signal of PMC are g_x = 6.28, g_y = 5.56, and g_z = 1.97 (Figure 1A) (Jouve et al., 1984), and similar spectrum has also been reported for MLC (Benecky et al., 1993). The EPR spectrum of the PMC sample treated with an excess of peroxyacetic acid (final solution pH 6.8, see Experimental Procedures) undergoes significative changes (Figures 1B and 2A). The characteristic EPR signal for the high-spin ferric hemes constituting the catalytic site practically disappeared, while a new, asymmetric signal in the $\mathbf{g}$ = 2 region appears. This signal, with broad wings, has its first derivative which crosses the baseline at $\mathbf{g} \simeq 2.01$ and ressembles the signal of HRP I (Schulz et al., 1979). This signal is also characterized by a fast longitudinal relaxation time, and its intensity is strongly reduced even at 10 K. We assign the PMC signal of Figure 1B to a porphyrin π-cation radical in exchange interaction with the oxoferryl moiety.

Figure 2 shows the pH effect on the shape of the EPR signal of PMC I in the $\mathbf{g}$ = 2 and $\mathbf{g}$ = 2.7 regions. At pH 6.8, the EPR spectrum observed for PMC I is dominated by an HRP I-type signal (Figure 1B) and named HpH I for high pH PMC I (Figure 2A). If the pH of the sample is lowered, the intensity of HpH I signal gradualy diminishes while a new broad (*ca.* 110 mT) EPR signal extending between *ca.* $\mathbf{g}$ = 3 and $\mathbf{g}$ = 2 (Figure 2) with two main resonances at $\mathbf{g}$ = 2.68 and $\mathbf{g}$ = 2.01 is observed. The shape of this signal, named LpH I for low pH PMC I, ressembles the signal detected for MLC I (Benecky et al., 1993). The relaxation properties of LpH I are not very different from those of HpH I, and above 10 K this form is hardly detected. In the intermediate range of pH, the two forms coexist (Figure 2B). During the titration, the sample retains its green color, which is indicative of the absence of changes in the redox state. At the lower pH attainable (pH 5.3), compatible with the stability of the protein (pI 4.8; Jouve et al., 1983), the transformation HpH I to LpH I is not complete, as indicated by the shape of the signal at $\mathbf{g} \simeq 2$ (Figure 2C). It is noteworthy that the changes between the two forms of PMC I were reversible with pH variations (results not shown). Moreover, the two pH-dependent forms of PMC I are present

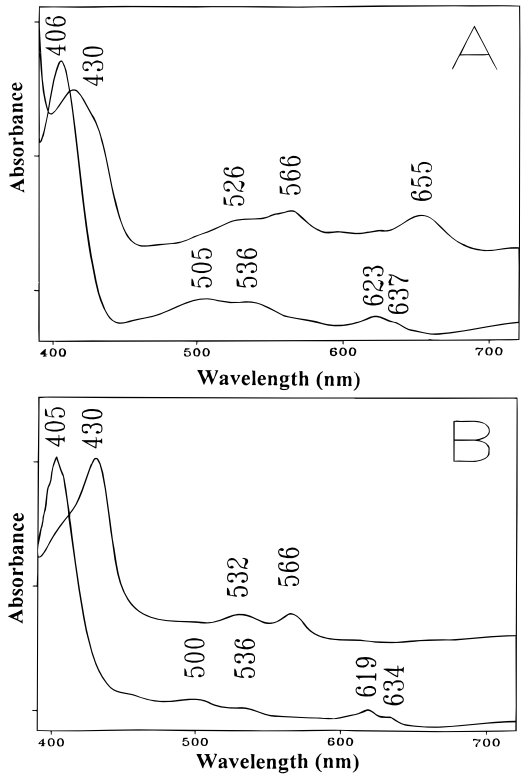

FIGURE 3: Low-temperature (10 K) absorption spectra of PMC (A) and BLC (B). Lower traces, native enzymes; upper traces, peroxyacetic acid-treated PMC (final pH 5.3) and BLC (final pH 5.6), for which the reaction was stopped at 15 s.

in either the NADPH-depleted PMC (A form) and the saturated form (B form, Jouve et al., 1989) (data not shown). Thus the change of the PMC I EPR signals appears to depend exclusively on the final pH of the sample.

Low-Temperature Electronic Absorption Spectrum of PMC and BLC Treated with Peroxyacetic Acid. The EPR spectrum of PMC I described in the previous section is typical of an oxoferryl coupled to a porphyrin π-cation radical (Figure 1) but differs from that of BLC (Ivancich et al., 1996), although in both cases the intermediate was formed by mixing native catalase with peroxyacetic acid at 0 °C and the reaction was stopped at 15 s. In order to verify if, in both cases, the electronic absorption spectrum well agrees with that of typical compound I (Deisseroth & Dounce, 1970), we performed low-temperature absorption measurements on samples of PMC and BLC, which were obtained using exactly the same protocol as for the EPR samples (see above).

The 10 K absorption spectra of native PMC (Figure 3A, lower trace) and native BLC (Figure 3B, lower trace) well agree with those reported at room temperature (Chance, 1952a; Jouve et al., 1984). The observed bands are the Soret band at 405 (406) nm, the bands at 500 (505) and 536 (536) and two other bands at 619 (623) nm and 634 (637) nm for BLC (PMC). Interestingly, the charge transfer band (630 nm) at room temperature is well resolved into two bands at 10 K.

The 10 K electronic absorption spectrum of PMC treated with peroxyacetic acid (Figure 3A, upper trace) shows the typical changes due to compound I formation (Gouet et al., 1996), that is a decrease and a broadening of the Soret band and a displacement of the charge transfer band at 655 nm. In addition, the other bands at 430, 526, and 566 nm are

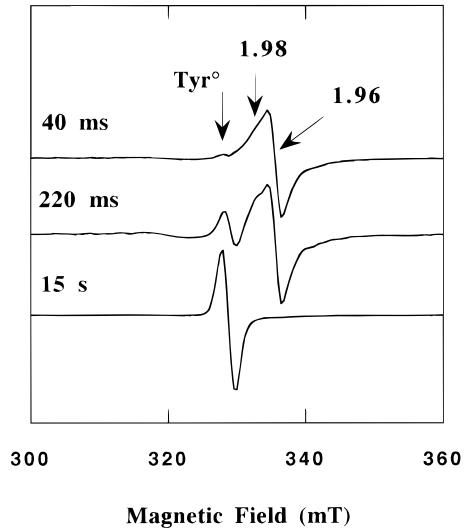

FIGURE 4: Reaction of BLC with peroxyacetic acid as monitored by the 4.2 K EPR spectra. The spectra were obtained on BLC samples for which the reaction was freeze−quenched at 40 ms, 220 ms, and 15 s. The experimental conditions were as in Figure 1 except that modulation amplitude was 0.1 mT.

indicative of formation of about 20% of compound II (Gouet et al., 1996). In contrast, the absorption spectrum of BLC in these conditions (Figure 3B, upper trace) only shows the typical pattern of the compound II absorption spectrum, i.e. absorption bands at 430, 532, and 566 nm.

Thus, the low-temperature absorption spectra on PMC treated with peroxyacetic acid (15 s reaction) indicate that PMC is predominantly in the compound I intermediate state, that is the oxoferryl moiety coupled with a porphyrin π-cation radical. This result fully agrees with the EPR spectrum of PMC I (Figure 1B). Under the same experimental conditions, BLC shows a compound II-type electronic absorption spectrum and the EPR spectrum indicates that the radical species arises from an amino acid residue, most likely a tyrosine (Ivancich et al., 1996).

EPR of BLC I. Rapid-Mix Freeze−Quench Evidence for the Formation of Porphyrin π-Cation Radical. The EPR signal of native BLC sample is typical of high-spin ferric heme as in PMC and was already described (Blum et al., 1978).

Figure 4 shows the EPR spectra at *ca.* $\mathbf{g} = 2$ of BLC samples treated with peroxyacetic acid and for which the reaction was stopped subsequently at 40 ms, 220 ms, and 15 s. As mentioned before, a tyrosyl radical is obtained at long mixing times (Figure 4C). It is noteworthy that the tyrosyl radical is saturated in the EPR conditions used to record the spectra of Figure 4. Nevertheless, under nonsaturating conditions it does show the previously reported proton hyperfine structure (Figure 5B). Spin quantification of the tyrosyl radical yields 0.8 spin/heme, indicating that it cannot be the result of a side reaction in BLC.

When the reaction of native BLC and peroxyacetic acid was stopped at 220 ms (final pH was 5.6), two other EPR signals could be observed (Figure 4, 220 ms). One of these, a broad (*ca.* 18 mT) and nearly symmetrical signal, at $\mathbf{g} \simeq 1.96$, has a short relaxation time and was hardly observed above 10 K (Figure 5A). The second, also symmetrical (Figure 4), at $\mathbf{g} \simeq 1.98$, could be also observed at 16 K although it shows a power saturation behavior which does not agree with that of an organic free radical (Figure 5A).

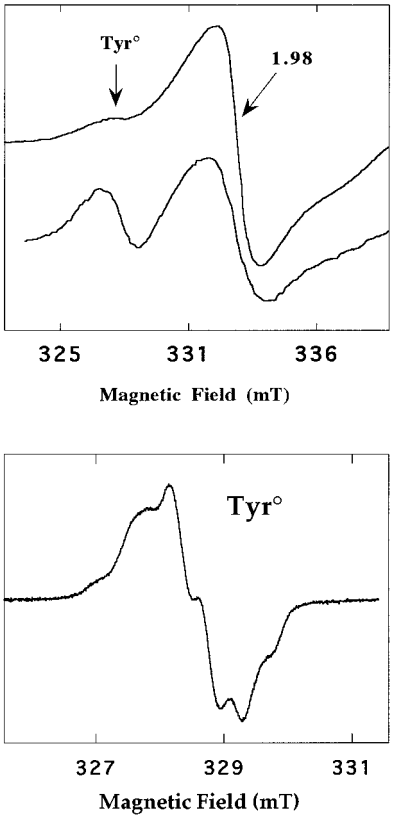

FIGURE 5: (A) Effect of microwave power on the EPR signal at **g** = 1.98 at 17 K. The spectra were obtained with BLC sample freeze−quenched at 40 ms (Figure 4). Upper trace, 10 mW; lower trace, 0.2 mW. Other experimental conditions were as in Figure 1. (B) EPR spectrum of the BLC tyrosyl radical at 86 K. The experimental conditions are as in Figure 4, except that a microwave power of 1 μW and a modulation amplitude of 0.16 mT were used.

These two signals were predominant when stopping the reaction at 40 ms (Figure 4), and both were not detected at freezing times longer than 15 s; in such conditions, only the tyrosyl radical was present (Figure 4, 15 s). No other signals were detected at lower field values, although the presence of broad signals, similar to those observed for LpH I (this study) or LiP I (Khindaria & Aust, 1996), cannot be formally excluded.

The signal at $\mathbf{g} \simeq 1.96$ has relaxation behavior very similar to the one observed for HpH I (Figure 2A), the latter was assigned to a porphyrin π-cation radical coupled to the oxoferryl iron from the heme active site (see above). The signal at $\mathbf{g} \simeq 1.98$ does not resemble any compound I intermediates in peroxidases or catalases. At 17 K, the $\mathbf{g} \simeq 1.96$ EPR signal of the sample frozen in 220 ms disappears and the $\mathbf{g} \simeq 1.98$ saturates differently from the tyrosyl radical at $\mathbf{g} \simeq 2.005$ (Figure 5A). These observations indicate that the relaxation behavior of the $\mathbf{g} \simeq 1.98$ signal is intermediate between that of an porphyrin π-cation radical and that of a free radical. Thus, we cannot exclude that this signal arises from the oxidation of an amino acid residue, close enough to the heme site so that it would be efficiently relaxed by the oxoferryl iron. But, in line with the results described above for PMC I, for which two coexisting species for Compound I are observed at pH 5.3, both species observed for BLC I (at $\mathbf{g} \simeq 1.96$ and $\mathbf{g} \simeq 1.98$) could rather be related to two pH-dependent conformations. The NADPH-saturated form of native BLC was used in this experiment, but similar results (data not shown) were obtained for NADPH-depleted BLC samples (Jouve et al., 1986).

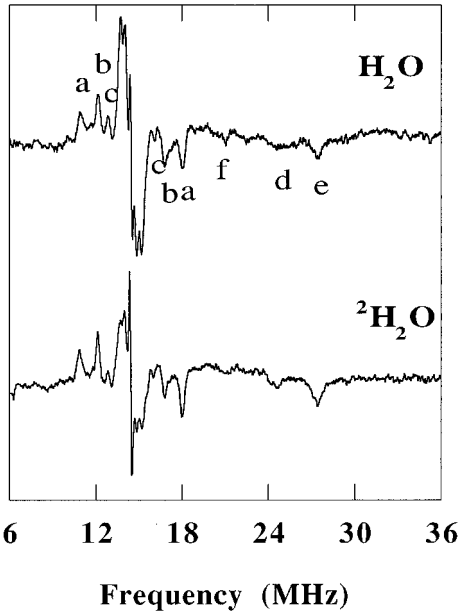

FIGURE 6: Proton ENDOR spectra of the BLC tyrosyl radical in frozen solution, incubated in ^1H_2O (upper trace) and ^2H_2O (lower trace). Experimental conditions: temperature, 5 K; microwave frequency, 9.469 GHz; magnetic field, 337.8 mT; modulation amplitude, 1.5 kHz; microwave power, 2 mW; RF modulation frequency, 110 kHz; time constant, 1.25 s; five scans.

The ENDOR Spectrum of the Tyrosyl Radical in BLC. Progressive power saturation studies on BLC protein radical have been already published (Ivancich et al., 1996), and a $P_{1/2}$ value of 0.060 mW at 20 K was found. This value has to be compared with a $P_{1/2}$ of 0.015 mW that we obtained with a free UV-generated tyrosyl radical examined at the same temperature. This comparison confirms that the BLC tyrosyl radical is relaxed by another paramagnetic species.

Figure 6 shows the ENDOR spectrum, at 5 K, of the BLC radical in fully protonated buffer (upper trace). The predominant resonances in the BLC ENDOR spectrum are those lines in the low- and high-frequency side of the free proton Larmor frequency. The three pairs of peaks at 10.9 and 18.0, 12.1 and 16.8, and 12.9 and 16.0 MHz (labeled aa, bb, and cc, respectively) well agree with the A_x, A_y, and A_z components of the rhombic tensor of the hyperfine couplings to the $C_{2,6}$ phenol ring protons reported for RNR and PSII tyrosyl radical (see Table 1 in Ivancich et al., 1996). The resonances at 12.9 and 16.0 MHz could also have contributions from (or alternatively, be assigned to) a purely dipolar coupled proton in the vicinity of the radical, as it was observed in the ENDOR spectrum of PSII $Tyr_{D(Z)}$ (Rigby et al., 1994; Tang et al., 1996).

Due to the strong similarity both in shapes and positions with the homologous signals observed for the RNR Tyr (Bender et al., 1989), two other relatively weak and broad resonances at 27.4 and 24.5 MHz (labeled d and e on Figure 6, upper trace) are assigned to the A_x and A_z hyperfine components of the $C_{3,5}$ phenol ring protons. The A_y component could be partially masked by the sharp intense transition at 18.0 MHz, as it was already observed in the RNR ENDOR spectrum (Bender et al., 1989).

Inspection of the spectrum in Figure 6 (upper trace) reveals the presence of at least one weak resonance at 21.0 MHz

Table 1: Experimental and Simulated Principal ^{1}H Hyperfine Tensor Values of the Tyrosyl Radical in Bovine Liver Catalase

ENDOR transitions[a]	ENDOR frequency (MHz)	hyperfine coupling (MHz)[b]	assignment[c]	hyperfine coupling (MHz)[d]
aa	10.8; 18.0	7.2	(2,6) A_y	7.0
bb	12.1; 16.7	4.6	(2,6) A_x	5.0
cc	12.9; 16.0	3.0	(2,6) A_z	<3.0
a	18.0	−7.2	(3,5) A_y	−7.2
d	24.4	−20.0	(3,5) A_z	−19.5
e	27.5	−26.2	(3,5) A_x	−25.9
f	21.0	13.2	β_2 A_{iso}	12.3
	(23.0)	(17.2)	β_1 A_{iso}	17.2

[a] Observed lines in the BLC ENDOR spectrum (see Figure 6). [b] This work; calculated as $A/2 = \nu_p \pm \nu$, being ν_p the proton Larmor frequency (14.4 MHz in our experimental conditions) since all A values verify the condition $|A/2| < \nu_p$. [c] Tensor axis definition and [d]estimated hyperfine couplings from the simulations of the BLC EPR spectrum taken from Ivancich et al. (1996).

(peak labeled f) and another even weaker line at 20 MHz. These peaks could be assigned to the hyperfine couplings to the β-methylene protons. They well agree with our previously estimated hyperfine couplings to the purported β-protons of the BLC tyrosyl radical, from which we would expect to observe resonances at *ca.* 20 and 22 MHz in the ENDOR spectrum (Table 1).

All the lines mentioned above and observed in the fully protonated ENDOR spectrum (Figure 6, upper trace) remain practically unchanged in the deuterium-exchanged BLC spectrum (Figure 6, lower trace), indicating that they originate from nonexchangeable protons as expected for proton couplings to a tyrosyl radical. The assignments of the observed frequencies in the ENDOR spectrum to the proton hyperfine couplings of the BLC radical, and a comparison with those couplings we previously proposed from the simulations of the EPR spectrum, are shown in Table 1.

The broad predominant feature of the ^{1}H ENDOR spectrum (Figure 6, upper trace) centered at *ca.* 14 MHz (Larmor frequency of the free protons) reflects the contributions from the weakly coupled protons in the vicinity of the tyrosyl radical. The intensity of this central line slightly decreases after deuteration of the BLC sample. This variation reflects the accessibility of the buffer to the BLC radical environment. Similar results were reported for the RNR (Bender et al., 1989) and PSII (Tommos et al., 1995) tyrosyl radicals.

DISCUSSION

The Porphyrin π-Cation Radical in PMC and BLC. Compound I of catalases has received much less attention than the corresponding intermediate state in peroxidases (Weiss et al., 1996; Poulos, 1996). The main reason may be due to the difficulty in stabilizing this intermediate state in enzymes with very fast turnover. However, the reaction with peroxyacetic acid instead of hydrogen peroxide considerably slows down the kinetics of the reaction. Only two EPR studies on catalase compound I have been undertaken, indicating quite different behavior for otherwise very similar enzymes. By EPR, an oxoferryl porphyrin π-cation radical was observed with MLC I (Benecky et al., 1993), but a tyrosyl radical was evidenced with BLC I (Ivancich et al., 1996).

The first important conclusion deduced from our results is the formation of compound I as the classical iron(IV)−oxoporphyrin π-cation radical in both PMC and BLC. PMC I is relatively stable and can be compared to the green MLC I. In contrast, BLC I is very short lived, only observable if the freeze−quench times are in the millisecond range.

The oxoferryl porphyrin π-cation radical has been described at length in HRP I as resulting from the magnetic coupling between the $S = 1$ spin of the oxoferryl moiety and the $S = {}^1/_2$ spin of the porphyrin π-cation radical (Dolphin et al., 1971; Schultz et al., 1979; Rutter et al., 1983). Interestingly, this coupling can be either ferromagnetic as observed in LiP I (Khindaria & Aust, 1996) and APX I (Patterson et al., 1995) or MLC I (Benecky et al., 1993) with the exchange coupling $J > 0$ or antiferromagnetic as observed in CPO I (Rutter et al., 1984) with $J < 0$. The EPR signals are well described in terms of the *J/D* parameter with D representing the zero field splitting parameter, generally the dominant term, of the order of 20 cm^{-1} or more. Depending on the sign of the exchange coupling, $\mathbf{g}_{eff}$ values have been calculated for the resulting ground spin state, $S = {}^3/_2$ or $S = {}^1/_2$, as a function of *J/D* (Rutter et al., 1984). We have used these plots to determine the nature of the coupling in both PMC I and BLC I.

In PMC two types of compound I are detected according to the pH value: the HpH I dominant at high pH and LpH I dominant at low pH. HpH I is characterized by an asymmetric signal whose first derivative absorption crosses the base line at $\mathbf{g}_{eff} \simeq 2.01$. Furthermore, this signal has a shape and relaxation properties very similar to HRP I considered as weakly AF coupled (Weiss et al., 1996). Because of these close similarities, we associated this signal to a weakly coupled oxoferryl porphyrin π-cation radical with a rather ferromagnetic characteristic as indicated by the effective apparent averaged $\mathbf{g}$ value slightly >2. As the pH of the solution is lowered, HpH I is continuously transformed into LpH I with a signal resembling closely that previously described for MLC I, an oxoferryl porphyrin π-cation radical with ferromagnetic character and a *J/D* paramater of the order of 0.3 (Benecky et al., 1993).

Modification of the exchange coupling within the same enzyme has never been reported before for other peroxidases where compound I is present exclusively under a single enzyme-dependent form. Varying the pH from high pH to low pH values reinforces the ferromagnetic character of PMC I.

In BLC, two species were also detected as transient intermediates in rapid freeze−quench experiments that gave signals in the $\mathbf{g} = 2$ region. One has $\mathbf{g}_{eff} \simeq 1.96$ and the other an averaged $\mathbf{g}_{eff}$ value closer to 2. The signal at $\mathbf{g} \simeq 1.96$ would have a rather AF character. On the basis of the EPR observations alone, the magnitude of the *J/D* parameter cannot be determined with absolute certainty, but in agreement with all experimental data on peroxidases, interpretation of the EPR signal in term of a weak *J/D* parameter seems the more likely. The second species may be considered as experiencing an also weak but definitively different exchange interaction, weaker than that of the $\mathbf{g} = 1.96$ species. Due to their different relaxation properties, they can be easily distinguished and related to two pH-dependent forms as those detected in PMC I. If the stronger ferromagnetic character of the interaction was the signature of the low pH form, as for PMC I, the $\mathbf{g} = 1.96$ signal would have to be associated

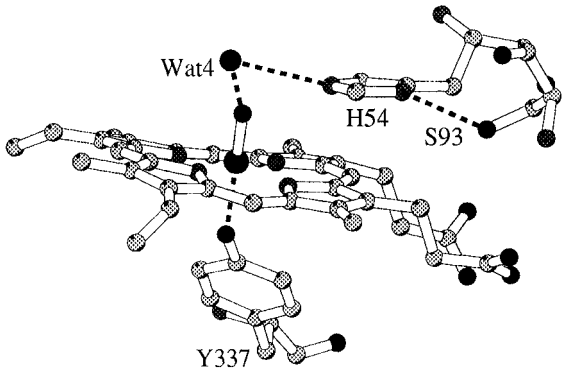

FIGURE 7: Active site of PMC I (from Gouet et al., 1996). On the distal site, the oxygen atom attached to the iron is represented with the water molecule (Wat4) situated at a distance less than 3 Å from the $N_\epsilon$of His 54 and from the former oxygen.

to HpH I. But, due to the instability of the oxoferryl porphyrin π-cation radical with time and the instability of native protein at low pH (pI 5.8) (Nicholls & Schonbaum, 1963), it was not possible to examine the pH variation effect on BLC I. Nevertheless, the important conclusion of this study is the presence of two forms for compound I, a situation very reminiscent of that found in PMC I.

The pH variations giving the EPR changes of PMC I are in the range 5−7 with a midpoint included between pH 5.3 and 6.0 (Figure 2). This value is close to the pK_a of an histidine. The structures of PMC and BLC are very conserved around the active site, in particular all of the histidines residues. On the distal side the essential histidine (His 54)[2] is present while on the proximal side two other histidine residues are very close to the heme: His 341 and His 197 (Gouet et al., 1995).

Structural results on PMC I (Gouet et al., 1996) show that on the distal side a water molecule (Wat 4 in Figure 7) close to the 6th coordination of the iron may be H-bound with His 54, conserved Asn 127, and the oxoferryl moiety. The protonation of His 54 at acid pH could modify this network of interactions around the active site and lead to the ferromagnetic character of LpH I. Raising the pH would have the opposite effect.

On the proximal side of the heme, His 197 and His 341 seem less accessible to the solvent (Gouet et al., 1995). Considering the residue His 197, the short distance found in the structure allows for the formation of a hydrogen bond between the N_ϵ of the imidazole ring and the guanidinium group of the conserved Arg 333, itself H-bound to the nearby phenolate proximal ligand (Tyr 337). The protonation of His 197 could weaken its binding with Arg 333. This would lower the "push" effect of the axial ligand (for the push−pull scheme, see Dawson, 1988) and then could rise the redox potential of the heme−phenolate couple, increasing the reactivity of compound I (Poulos, 1996; Goodin, 1996; Gross, 1996). His 341, H-bound to the propionate group of the heme is also an interesting residue because it belongs to the proximal helix (α9, Gouet et al., 1995), recently suggested to have a structural influence on compound I (Poulos, 1996). Protonation of His 341 at acid pH would increase this interaction with the propionate group and change the local symetry around the iron, producing the more ferromagneticaly coupled state of PMC I. However, it is not excluded that the pH effect on PMC I is due to the influence of all three histidyl residues mentioned above.

An effect of pH giving two EPR signals of different rhombicity (**g** tensor anisotropy) in native high-spin ferric heme state ($S = {}^5/_2$) of PMC or BLC has been also observed in the same range of pH values than with compound I (Blum et al., 1978; Jouve et al., 1984). A midpoint of pH 6.2 was determined with PMC and interpreted as changes in protonation of distal His 54. The approximate value of the midpoint corresponding to the changes of compound I EPR signals observed here seems weakly more acidic, perhaps due to an higher electropositivity of compound I.

Nevertheless, our results show, for the first time, that a slight pH variation can modulate the nature of the spin coupling between the oxoferryl and the porphyrin π-cation radical in enzymatic compound I. The nature of the spin coupling has been discussed recently (Weiss et al., 1996). Our results strongly emphasize the role of subtile modifications in the network of hydrogen bonds in the vicinity of the heme in inducing such changes. A mecanism of this type could explain the AF character of CPO I. Furthermore, it has been found that at low pH (below 5.0) the transition from compound I to compound II was accelerated in catalases (Chance, 1952b). The oxoferryl porphyrin π-cation radical with the most pronounced ferromagnetic character, the LpH I form favored at acid pH, could be considered as being the first step in the one-electron reduction of compound I.

The Tyrosyl Radical in BLC. This work emphasizes that, among catalases studied so far, BLC is unique since it stabilizes not only a transient porphyrin π-cation radical but also a protein radical. We have recently shown that the EPR signal of the BLC protein radical strongly resembles that of the PSII tyrosyl radicals and can be satisfactorily simulated by using proton hyperfine couplings that well agree with those of other tyrosyl radicals (Ivancich et al., 1996). The ENDOR spectrum of BLC constitutes further experimental evidence for such proposal since the hyperfine coupling tensors for the phenol ring protons do confirm the previously estimated values (Table 1). The resonances assigned to the β-methylene proton hyperfine couplings are very weak in our spectrum but nevertheless indicate that the β-protons are more symmetrically positioned ($\theta_1 = 57°$ and $\theta_2 = 63°$) than those reported for the PSII (Babcock et al., 1989; Debus, 1992) or the RNR (Bender et al., 1989; Un et al., 1995; Hoganson et al., 1996) tyrosyl radicals.

In the compound I of all peroxidases characterized so far, the second electron is removed from a porphyrin orbital with two noticeable exceptions: a mutant of HRP and wild-type CcP. In HRP, where Phe 172 (positioned on the proximal side of the heme) was mutated to a tyrosine residue, an unstable compound I was formed with a porphyrin cation radical together with a radical on Tyr 172 (Miller et al., 1995). However, contrary to what is observed in BLC, the protein radical represents only a minor component in the mutated HRP (about 10%).

In CcP I (Sivaraja et al., 1989; Huyett et al., 1995), the radical species originates from a tryptophan residue (Trp 191) which is very close to the histidine axial ligand. CcP I is characterized by its red color, corresponding to the oxoferryl moiety of Compound II and by an EPR signal for the protein radical. This situation is similar for BLC frozen after 15 s

[2] The numbering code used for the amino acid residues is that of the PMC sequence; the corresponding numbering in BLC is obtained by adding 20.

which presents the optical spectrum of Compound II and an EPR signal of a tyrosyl radical. An important difference must be pointed out: in CcP, no porphyrin radical was detected as precursor of the protein radical within the shortest time used for the formation of compound I (30 s, Patterson et al., 1995). In BLC, the reaction is clearly a two-step process, and we have demonstrated that the short-lived porphyrin radical was first formed followed by the tyrosyl radical. From these results and the very fast turnover of the enzyme on H_2O_2, it seems unlikely that the tyrosine radical would play a significant role in the catalatic function of the catalase.

In the BLC sequence, 20 tyrosine residues are present but only six are at distances smaller than 19 Å from the heme (Fita & Rossmann, 1985). The closest tyrosine on the proximal side of the heme has a iron−phenol oxygen distance of 1.8 Å. At such a distance, relatively strong magnetic interactions, of dipolar and (or) exchange origins, would occur between the electronic spin $S = 1$ of the oxoferryl moiety and the spin of the tyrosyl radical supposed to be located at this proximal site. Only a moderate relaxation rate acceleration, indicative of weak dipolar interactions, is noticed at the tyrosyl radical of BLC. On this ground, the possibility for the tyrosyl radical to be located at the Tyr 357 position can be excluded. Furthermore, the resonance Raman experiments (Chuang & Van Wart, 1992) do not show any frequency changes of the vibrational modes assign to the the iron−phenol oxygen bond between compound I and compound II as it would be expected if such tyrosine became oxidized.

An electron transfer from NADPH to the heme iron through the protein has been proposed to take into account the oxidation of the NADPH by catalases binding this cofactor. Furthermore, it has been postulated that NADPH does not react directly with compound I or compound II but with a new intermediate the so-called compound II* (Hillar et al., 1994). This intermediate would result from the decay of compound I and would be a protein radical, probably a tyrosyl. On the basis of our results, the tyrosyl radical observed simultaneously with the oxoferryl moiety in BLC could well correspond to this hypothetical compound II*.

On the basis of the crystal structure of BLC, the possible electron pathways between NADPH and the heme have been simulated (Olson & Bruice, 1995), and one probable pathway involves Tyr 214. This tyrosine could be implicated in the radical formation. Moreover, it was demonstrated that one of the two most probable pathways in PMC involves Phe 194 homologous to Tyr 214 of BLC (Bicout et al., 1995). The absence of a tyrosyl radical in PMC would agree with such a substitution. However, a tyrosine is also present in MLC at this particular position while no radical was detected in MLC I (Benecky et al., 1993). Consequently, another tyrosine residue (Tyr 235 of BLC) also involved in the electron transfer pathways (Olson & Bruice, 1995) has been considered. This tyrosine is substituted by a phenylalanine in both MLC and PMC and could host the tyrosyl radical in BLC. With regard to the other three tyrosines (Tyr 136, 324, and 369 of BLC), only Tyr 369 is not conserved in PMC and MLC and could also be involved. We must, however, keep in mind that other factors could influence the reactivity of any given tyrosine residue. It has been established, in CcP I (Bonagura et al., 1996) and APX I (Pappa et al., 1996), that long-range electrostatic effects generated by ionic ligand could play an important role on the radical stability. Interestingly, an unidentified anion binding site has been observed in PMC I (Gouet et al., 1996). Site-directed mutagenesis experiments are in progress on PMC to help choose between these different hypotheses.

ACKNOWLEDGMENT

We are grateful to Drs. Tony A. Mattioli and Yves Dupont for the use of the Cary absorption spectrometer and the MIXCON freeze−quench apparatus, respectively. We are indebted to Dr. Patrice Gouet for fruitful discussions on PMC structure and for the realization of Figure 7 and Dr. J. Gagnon for a careful reading of the manuscript. We thank Drs. Klaus Brettel, A. William Rutherford, Andreas Seidler, and Sun Un for stimulating discussions, as well as Gerard Desfonds for his expert technical support.

REFERENCES

Appleyard, R. J., Shuttleworth, W. A., & Evans, J. N. S. (1994) *Biochemistry 33*, 6812−6821.
Babcock, G. T., Barry, B. A., Debus, R. J., Hoganson, C. W., Atamian, M., McIntosh, L., Sithole, I., & Yocum, C. F. (1989) *Biochemistry 28*, 9557−9565.
Bender, C. J., Sahlin, M., Babcock, G. T., Barry, B. A., Chandrashekar, T. K., Salowe, S. P., Stubbe, J., Lindström, B., Petersson, L., Ehrenberg, A., & Sjöberg, B.-M. (1989) *J. Am. Chem. Soc. 111*, 8076−8083.
Benecky, M. J., Frew, J. E., Scowen, N., Jones, P., & Hoffman, B. M. (1993) *Biochemistry 32*, 11929−11933.
Bicout, D. J., Field, M. J., Gouet, P., & Jouve, H. M. (1995) *Biochem. Biophys. Acta 1252*, 172−176.
Blum, H., Chance, B., & Litchfield, W. J. (1978) *Biochem. Biophys. Acta 534*, 317−321.
Bonagura, C. A., Sundaramoorthy, M., Pappa, H. S., Patterson, W. R., & Poulos, T. L. (1996) *Biochemistry 35*, 6107−6115.
Bravo, J., Fita, I., Gouet, P., Jouve, H. M., Melik-Adamyan, W., & Murshudov, G. N. (1997) in *Oxidative Stress and The Molecular Biology of Antioxidant Defenses* (Scandalios, J. G., Ed.) pp 407−445, Cold Spring Harbor Laboratory Press, New York.
Buzy, A., Bracchi, V., Sterjiades, R., Chroboczek, J., Tibault, P., Gagnon, J., Jouve, H. M., & Hudry-Clergeon, G. (1995) *J. Protein Chem. 14*, 59−72.
Chance, B. (1952a) *Arch. Biochem. Biophys. 41*, 404−415.
Chance, B. (1952b) *J. Biol. Chem. 194*, 471−481.
Chance, B., Sies, H., & Boveris, A. (1979) *Physiol. Rev. 59*, 527−605.
Chuang, W.-J., & Van Wart, H. E. (1992) *J. Biol. Chem. 267*, 13293−13301.
Dawson, J. H. (1988) *Science 240*, 433−439.
Debus, R. J. (1992) *Biochem. Biophys. Acta 1102*, 269−352.
Deisseroth, A., & Dounce, A. L. (1970) *Physiol. Rev. 50*, 319−375.
Dolphin, D., Forman, A., Borg, D. C., Fajer, J., & Felton, R. H. (1971) *Proc. Natl. Acad. Sci. U.S.A. 68*, 614−618.
Fita, I., & Rossmann, M. G. (1985) *J. Mol. Biol. 185*, 21−37.
Goodin, D. B. (1996) *J. Biol. Inorg. Chem. 1*, 360−363.
Gouet, P., Jouve, H. M., & Dideberg, O. (1995) *J. Mol. Biol. 249*, 933−954.
Gouet, P., Jouve, H. M., Williams, P. A., Andersson, I., Andreoletti, P., Nussaume, L., & Hajdu, J. (1996) *Nature Struct. Biol. 3*, 951−956.
Gross, Z. (1996) *J. Biol. Inorg. Chem. 1*, 368−371.
Halliwel, B., & Gutteridge, J. M. C. (1984) *J. Biochem. 219*, 1−14.
Hillar, A., & Nicholls, P. (1992) *FEBS Lett. 314*, 179−182.
Hillar, A., Nicholls, P., Switala, L., & Lowen, P. C. (1994) *Biochem. J. 300*, 531−539.
Hoganson, C. W., Sahlin, M., Sjöberg, B.-M., & Babcock, G. T. (1996) *J. Am. Chem. Soc. 118*, 4672−4679.
Huyett, J. E., Doan, P. E., Gurbiel, R., Houseman, A. L. P., Sivaraja, M., Goodin, D. B., & Hoffman, B. M. (1995) *J. Am. Chem. Soc. 117*, 9033−9041.

Ivancich, A., Jouve, H. M., & Gaillard, J. (1996) *J. Am. Chem. Soc. 188*, 12852−12853.
Jones, P., & Middlemiss, D. N. (1972) *Biochem. J. 130*, 411−415.
Jouve, H. M., Tessier, S., & Pelmont, J. (1983) *Can. J. Biochem. Cell Biol. 61*, 8−14.
Jouve, H. M., Gaillard, J., & Pelmont, J. (1984) *Can. J. Biochem. Cell Biol. 62*, 935−944.
Jouve, H. M., Pelmont, J., & Gaillard, J. (1986) *Arch. Biochem. Biophys. 248*, 71−79.
Jouve, H. M., Beaumont, F., Léger, I., Foray, J., & Pelmont, J. (1989) *Biochem. Cell Biol. 67*, 271−277.
Khindaria, A., & Aust, S. D. (1996) *Biochemistry 35*, 13107−13111.
Kirkman, H. N., Galiano, S., & Gaetani, G. F. (1987) *J. Biol. Chem. 262*, 660−666.
Lardinois, O. M. (1995) *Free Rad. Res. 22*, 251−274.
Miller, V. P., Goodin, D. B., Friedman, A. E., Hartmann, C., & Ortiz de Montellano, P. R. (1995) *J. Biol. Chem. 270*, 18413−18419.
Moulis, J.-M., Davasse, V., Meyer, J., & Gaillard, J. (1996) *FEBS Lett. 380*, 287−290.
Nicholls, P., & Schonbaum, G. R. (1963) in *The Enzymes* (Boyer, P. D., Lardy, H., & Myrbäck, K., Eds.) Vol. 8, pp 147−225, Academic Press, New York.
Olson, L. P., & Bruice, T. C. (1995) *Biochemistry 34*, 7335−7347.
Pappa, H., Patterson, W. R., & Poulos, T. L. (1996) *J. Biol. Inorg. Chem. 1*, 61−66.
Patterson, W. R., Poulos, T. L., & Goodin, D. B. (1995) *Biochemistry 34*, 4342−4345.
Poulos, T. L. (1996) *J. Biol. Inorg. Chem. 1*, 356−359.
Rigby, S. E. J., Nugent, J. H. A., & O'Malley, P. J. (1994) *Biochemistry 33*, 1734−1742.
Rutter, R., Valentine, M., Hendrich, M. P., Hager, L. P., & Debrunner, P. G. (1983) *Biochemistry 22*, 4769−4774.
Rutter, R., Hager, L. P., Dhonau, H., Hendrich, M., Valentine, M., & Debrunner, P. (1984) *Biochemistry 23*, 6809−6816.
Samejima, T., & Yang, J. T. (1963) *J. Biol. Chem. 238*, 3256−3261.
Schonbaum, G. R., & Chance, B. (1976) in *The Enzymes* (Boyer, P. D., Ed.), Vol. 13, pp 363−408, Academic Press, New York.
Schulz, C. E., Devaney, P. W., Winkler, H., Debrunner, P. G., Doan, N., Chiang, R., Rutter, R., & Hager, L. P. (1979) *FEBS Lett. 103*, 102−105.
Sivaraja, M., Goodin, D. B., Smith, M., & Hoffman, B. M. (1989) *Science 245*, 738−740.
Tang, X., Zheng, M., Chisholm, D. A., Dismukes, G. C., & Diner, B. (1996) *Biochemistry 35*, 1475−1484.
Tommos, C., Tang, X.-S., Warncke, K., Hoganson, C. W., Styring, S., McCracken, J., Diner, B., & Babcock, G. T. (1995) *J. Am. Chem. Soc. 117*, 10325−10335.
Un, S., Atta, M., Fontecave, M., & Rutherford, A. W. (1995) *J. Am. Chem. Soc. 117*, 10713−10719.
Vuillaume, M. (1987) *Mut. Res 186*, 43−72.
Weiss, R., Mandon, D., Wolter, T., Trautwein, A. X., Müther, M., Bill, E., Gold, A., Jayaraj, K., & Terner, J. (1996) *J. Biol. Inorg. Chem. 1*, 377−383.

BI970886S